

## The classical phase space for quantum dots

M. Stopa

*The Tarucha Mesoscopic Correlation Project, ERATO-JST  
4S-308S NTT Atsugi Research and Development Laboratories  
3-1 Morinosato Wakamiya, Atsugi shi  
Kanagawa ken, 243-0198, Japan  
stopa@tarucha.jst.go.jp*

### Abstract

We numerically integrate Hamilton's equations for the classical phase space trajectories of electrons confined in a closed quantum dot. The dot potential contour is obtained numerically via full, 3D spin density functional calculations of a realistic, GaAs-AlGaAs heterostructure based device. We show that the phase space of the dot is mixed and, as a function of increasing energy, becomes increasingly chaotic. We show that this is related to the well-screened, symmetric shape of the potential at low energies and the un-screened, irregular perimeter shape at the Fermi surface. We employ an iterative method to search for periodic orbits in the dot, employing the computed matrixant.

### Introduction

Considerable progress in understanding chaos in Hamiltonian systems has been made by employing numerical methods in the study of classical behavior in billiards and other artificial potentials<sup>1</sup>. In particular, the field of "semiclassical physics" seeks to interpret phenomena which are observed or calculated in quantum systems by referring to the classical periodic orbits in some assumed confining potential for the system<sup>2</sup>. One system to which semi-classical methods have been applied recently is the quantum dot. Quantum dots, also known as "artificial atoms," are islands of electrons in semiconductor heterostructures which are isolated by means of metal gates placed on the surface of the semiconductor wafer. Frequently the electrons, and hence the quantum dots are effectively two dimensional due to the confining of the electrons at the interface between two types of semiconductor material (e.g. GaAs and AlGaAs).

Electron-electron interactions in quantum dots are responsible for many of their experimentally observed characteristics. However, in classical physics, electron-electron interactions, if they are considered at all, are included explicitly as an interaction term in the Hamiltonian. Therefore, except for a very small number of electrons ( $N=3$  or  $4$ ), the dynamics of an interacting system become intractable for even large computers. By contrast, when billiard calculations are applied to quantum dots, it is generally assumed that the electrons move in some mean field potential, which is unchanging (throughout the particular experiment under consideration). The reason for this independent electron assumption is simply that quantum dots can typically contain a large number of electrons  $N^3$ . Hence no other approach is feasible.

Recently, we have shown, using spin density functional (SDF) theory for the self-consistent electronic structure of quantum dots, that fluctuations in the energy required to add an electron to the dot, the so-called "addition spectrum," were partially attributable to

particular “scar-like” wavefunctions in the spectrum<sup>4</sup>. These eigenfunctions exhibited a distinctly one-dimensional character and were concentrated along 1D paths, in contrast to the majority of the dot eigenstates which more or less homogeneously spread through the entire, 2D dot area. Furthermore, sequences of states at differing energies were found to concentrate along the same path or trajectory, with an additional node in the wavefunction for each successive state. Since the Coulomb interaction falls off as  $1/|\mathbf{r}_1-\mathbf{r}_2|$ , where  $\mathbf{r}_1$ ,  $\mathbf{r}_2$  are the positions of electrons 1 and 2, the Coulomb interaction of two eigenfunctions which concentrate along the same trajectory was found to be significantly enhanced relative to that of two, homogeneously distributed wavefunctions. The consequences of interaction were also significant for the *spin* of the quantum dot. For two electrons in the same, quasi-1D orbital, the interaction is particularly enhanced. Thus, the filling of two successive spin states of such a “scarred” wavefunction is strongly inhibited. This leads to a tendency toward spontaneous spin polarization<sup>5</sup>.

In this paper, we present the results of a study of the classical phase space of a quantum dot whose effective 2D confining potential,  $V(x,y)$ , is calculated self-consistently, taking into account the dot electrons, the positive background donor charges, the composition profile of the semiconductor wafer in which the dot is fabricated, and the locations and voltages on the surface gates which deplete the surrounding two dimensional electron gas (2DEG) and form the quantum dot. We solve Hamilton’s equations for classical trajectories. A Poincaré surface of section is defined as the vertical midline through the dot, taking only trajectories which are passing from left to right (see Figure 1). Furthermore, we numerically compute the “matrizant,” which gives a linear approximation to the evolution of the separation between two trajectories. Using a method developed by Blaschke<sup>6</sup>, the matrizant is employed in an iterative procedure to locate both stable and unstable periodic orbits of the dot.

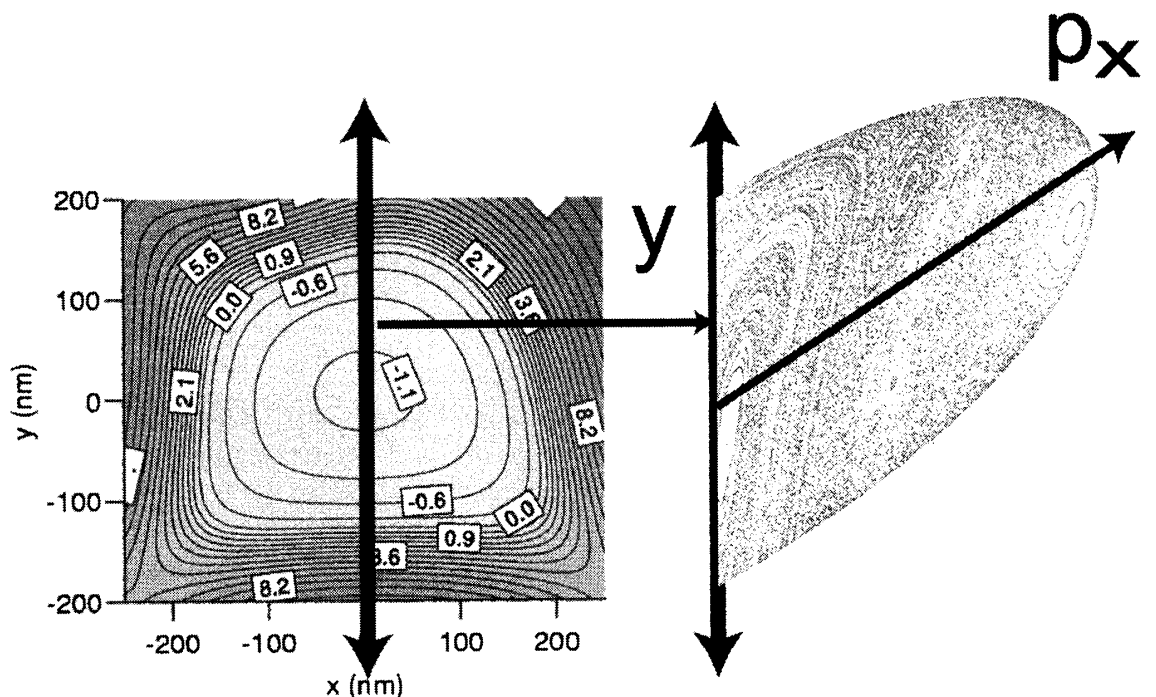


**Figure 1** Effective 2D potential contour  $V(x,y)$  of quantum dot. Potential contours labeled in  $Ry$  ( $1 Ry \approx 5.8 meV$ ), Fermi surface at  $V=0$ . Schematic shows definition of Poincaré surface of section (SOS), chosen as line that bisects dot (typically  $x=0$ ) and  $x$ -component of momentum as

electrons cross from left to right (hence always positive). Also, only points with  $p_y < 0$  chosen;  $p_y > 0$  forms another branch of SOS.

### Calculation

Our spin density functional calculations for the electronic structure of lateral semiconductor quantum dots have been described in the literature in detail<sup>7</sup>. Here, we are only concerned that the effective, 2D confining potential of electrons in the dot,  $V(x,y)$ , is computed numerically and self-consistently; taking into account all of the (3D) geometrical features of the structure and in addition the charge density of the electrons occupying the dot. The structure which we use here is our model of the dot fabricated by Sivan *et. al.*<sup>8</sup> and has a lithographic diameter of approximately  $\frac{1}{2} \mu\text{m}$  and contains approximately  $N \sim 100$  electrons. The contour,  $V(x,y)$ , is shown in figure 1. The dot is connected via quantum point contact leads, in the lower left and lower right corners, to wide regions of 2DEG, which serve as the source and the drain in transport through the dot. The saddle point potentials to the leads are above the Fermi surface ( $V=0$  in the figure) and therefore electrons must quantum mechanically tunnel into and out of the dot.

The calculated self-consistent potential (Fig. 1) can be used to calculate classical orbits in the quantum dot as a function of the orbit energy  $E$ . For a fixed, 2D potential  $V(x,y)$ , Hamilton's equations for the classical motion of an electron can be written in symplectic form:

$$\frac{d\eta}{dt} = \mathbf{J} \frac{\partial H}{\partial \eta}$$

where  $\eta \equiv (\mathbf{p}, \mathbf{x})$  is the position of the electron in 4D phase space and where

$$\mathbf{J} \equiv \begin{pmatrix} \mathbf{0} & \mathbf{1} \\ -\mathbf{1} & \mathbf{0} \end{pmatrix}.$$

Here,  $\mathbf{0}$  and  $\mathbf{1}$  are  $2 \times 2$  zero and unit matrices, respectively. The Hamiltonian for the system is simply  $H(\mathbf{p}, \mathbf{x}) = \mathbf{p}^2 + V(\mathbf{x})$  (in units where  $2m=1$ ). Simultaneous with the numerical integration of Hamilton's equations, we also obtain the matrizant, which is defined as:

$$\delta\eta(t) = \chi(t - t_0) \delta\eta(t_0)$$

where  $\delta\eta$  is the 4-vector deviation of two trajectories in phase space. The matrizant obeys the equation<sup>6</sup>

$$\frac{d\chi(t)}{dt} = \mathbf{J} \frac{\partial^2 H}{\partial \eta^2} \chi(t).$$

Note that the matrizant is a  $4 \times 4$  matrix and hence we must integrate the sixteen components at the same time. Also note that the matrizant gives only a linear relationship between the deviation of two trajectories as a function of time.

The reason for computing the matrizant is that it can be used to formulate an iterative procedure for finding the periodic orbits. Given an arbitrary trajectory, which begins at  $\eta_i$  on the SOS and ends at  $\eta_f$  (which is also on the SOS, approaching from the left, after some integer number of passes through, from left to right), it is straightforward to show that the new initial point  $\eta'_i = \eta_i + (1 - \chi(T))^{-1} (\eta_f - \eta_i)$  is that of a periodic orbit.

Here  $T$  is the time to go from  $\eta_i$  to  $\eta_f$ . It is actually necessary to iterate this procedure

numerically. This is because of the linear approximation made in the definition of the matrizant. Note that the matrizant, evaluated at the period of a periodic orbit, is identical to the so-called “monodromy matrix.”

### Results

The Poincaré SOS can be defined in various ways, depending on the problem. The main point is to reduce the number of degrees of freedom of the system to two and plot the points where the trajectories of the system pass, quasi-periodically, through the surface. In our case, we choose a bisecting line (typically the  $y$ -axis) and calculate numerically points where trajectories pass through from a given direction (in our case, from negative to positive  $x$ ). The second coordinate is the momentum in the  $x$ -direction (see Figure 1 caption). There is a further ambiguity which is resolved by choosing only those points which have a  $y$ -component of momentum with a given sign.

The principal result, which we emphasize here, is that the phase space of the dot is of the “mixed” variety, having large chaotic regions and small islands of stability. Furthermore, as the energy increases from the bottom of the potential, figure 2, the regions of stability become smaller. Even for energies that are below the Fermi surface of the dot, we see that most of the stable regions have become unobservable at the scale of the plot in figure 2. The reason for the evolution of the stability is seen in figure 1. For very small energies, near the bottom of the dot potential, the shape of the confinement can be approximated as elliptical or even circular parabolic. This results from the self-consistent nature of the potential and the screening property of the mobile electrons in the dot. However, as the energy increases, the orbits traverse regions closer to the boundary of the dot. Due to the electrostatic gating that forms the dot, these regions are irregularly shaped. Therefore, while there remain periodic orbits (indeed, they increase in number), they become more unstable and the elaborate fixed points seen at lower energy disappear.

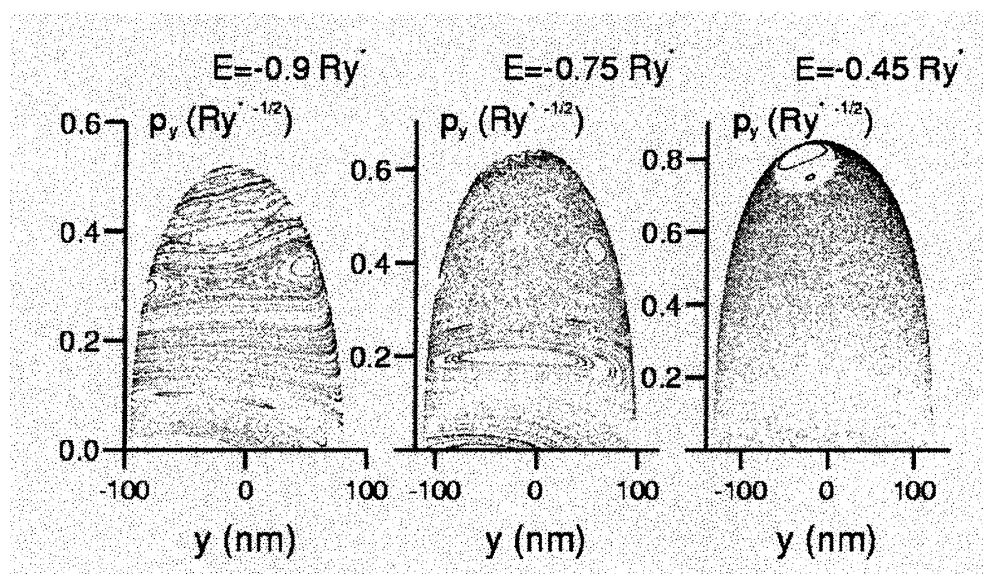


**Figure 2** Poincaré surfaces of section for various energies below the Fermi surface, calculated from the numerical integration of Hamilton's equations with the self-consistent potential illustrated in figure 1.  $E=0$  defines the Fermi surface of the dot. As electron energy increases, orbits impinge on the boundary of the dot which is very irregular. At lower energies, screening of the dot electrons results in a smooth, circular parabolic shaped potential which is nearly integrable.

In figure 3 we illustrate some of the periodic orbits, which are located by using the matrizant, as described above. Note that most of the orbits shown in figure 3 are stable, even though the energy is very close to the Fermi surface. Therefore, even though the SOS plots show a shrinkage of the regular regions of phase space, many of the stable orbits remain. As energy increases we find (not shown) that the orbits bifurcate and produce typically pairs of stable and unstable orbits.

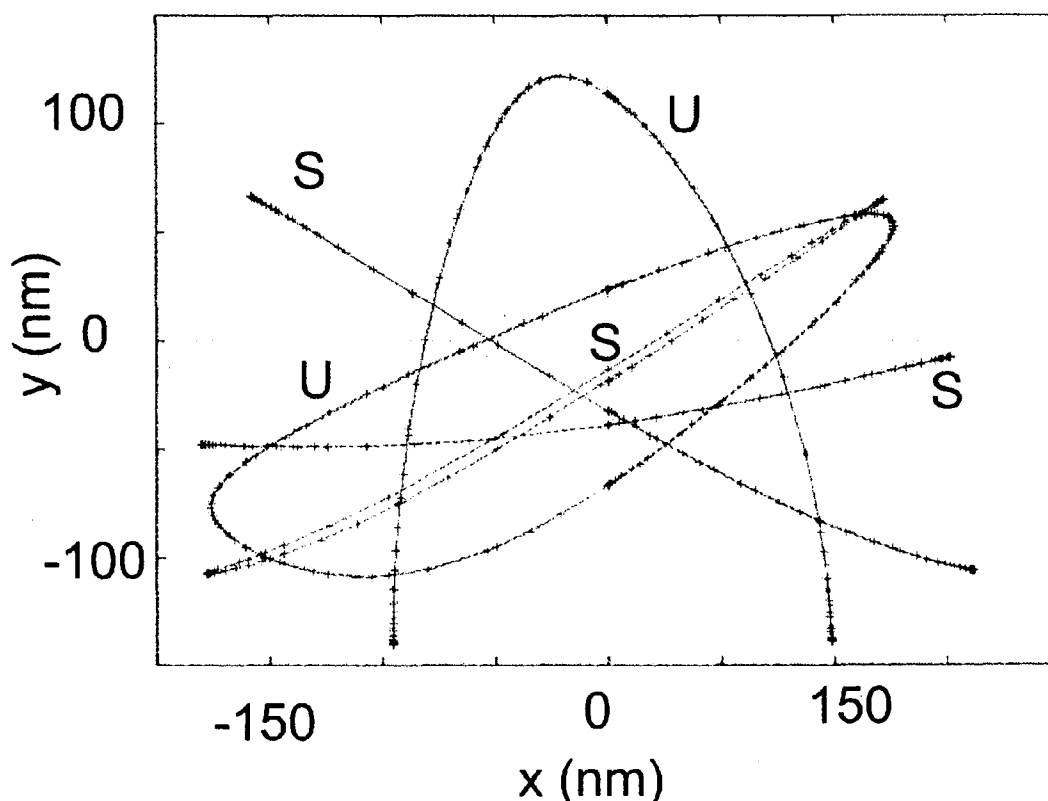


**Figure 3** Real space trajectories of several simple periodic orbits in the confining potential shown in figure 1. Orbits labeled with U are unstable and those with S are stable.

In addition to the orbit trajectories in real space, each orbit is characterized by its action, its period and its Maslov index (topological winding number). Finally, the monodromy matrix, which measures the rate of separation of nearby trajectories, is related to the stability of the orbit. In particular, in two dimensions, the trace of the reduced monodromy matrix (with the directions along the trajectory and perpendicular to the energy surface removed) signifies that an orbit is stable or unstable. This stability criterion is related to the nature of the fixed point in the Poincaré SOS.

### Conclusions

In this short paper we have investigated the classical phase space of electrons confined to a lateral, semiconductor quantum dot. The potential profile for the dot is obtained from full, self-consistent electronic structure calculations. A principal conclusion that we have reached is that the phase space is mixed and that the regions of chaos become increasingly dominant as the energy approaches the Fermi surface. The origin of this effect is the screening of the potential and the resulting, parabolic symmetry

arising from the screening of the gate potential by the dot electrons. Closer to the Fermi surface, the effects of the irregular shaped walls of the dot are stronger, and the orbits consequently become less regular. Further comparisons of the classical orbits with the eigenfunctions of the dot, and their relationship with the fluctuations of the charging energy will be presented in a future publication.

---

<sup>1</sup> See, for example, L. Kaplan, Phys. Rev. E **62**, 3476 (2000) and references therein.

<sup>2</sup> See M. Brack and R. K. Bhaduri, *Semiclassical Physics*, (Addison-Wesley, Reading 1997), for a general introduction to the physics of semiclassical systems.

<sup>3</sup> While quantum dot sizes vary considerably and quantum dots are now fabricated with as few as one electron, many relevant experiments are performed in the regime where  $N \sim 50-100$ .

<sup>4</sup> M. Stopa, Physica B, **249-251**, 228 (1998).

<sup>5</sup> M. Stopa, Semicond. Sci. Technol. **13**, A55 (1998).

<sup>6</sup> See, for example, J. Blaschke and M. Brack, Physica E **1**, 288 (1997).

<sup>7</sup> M. Stopa, Phys. Rev. B **54**, 13767 (1996); M. Stopa, Physica E **10**, 103 (2001).

<sup>8</sup> U. Sivan *et. al.*, Phys. Rev. Lett. **77**, 1123 (1996).